JOURNAL OF MATERIALS SCIENCE 24 (1989) 4315–4323

Size and temperature dependence of thermoelectric power and electrical resistivity of vacuum-deposited antimony thin films

V. DAMODARA DAS, N. SOUNDARARAJAN
Thin Film Laboratory, Department of Physics, Indian Institute of Technology, Madras 600 036, India

Thin antimony films of thicknesses in the range 30 to 200 nm have been vacuum deposited on glass substrates at room temperature. After annealing for about an hour at 500 K, the thermoelectric power and electrical resistivity were measured in vacuum as a function of temperature. The thermoelectric power and electrical conductivity data were combined and simultaneously analysed using the effective mean free path theory of size effect in thin films developed by Tellier and Pichard *et al.* In addition, their temperature dependence was also analysed. It was found that the thermoelectric power is positive and increases with increasing temperature and is inversely proportional to the thickness of the film. The electrical resistivity was found to be temperature dependent with the temperature coefficient of resistivity being positive, and inversely proportional to the thickness of the film. Analysis combining the data from the thermoelectric power and electrical conductivity measurements has led to the determination of mean free path, carrier concentration, effective mass, Fermi energy and the parameter $U_g = (\mathrm{d} \ln l_g / \mathrm{d} \ln E)_{E=E_F}$. The data were analysed for least squares fitting by local functions, such as the spline functions, which eliminates possible errors in conventional least squares fitting of data using non-local functions valid throughout the range.

1. Introduction

Antimony, a group V element, like bismuth, is a semimetal, having low, but degenerate, carrier concentration and the carriers have a low effective mass. It is well known that the structure can influence the semimetallic and semiconducting behaviour. The crystal structure of antimony, like that of bismuth, is rhombohedral with two pentavalent atoms in each unit cell. The rhombohedral lattice can be viewed as a distorted cubic lattice. This results in anisotropy in electrical and thermal properties. A fair amount of electrical conduction studies on antimony thin films has been carried out. Harris and Shaffer [1] reported some measurements on the electrical resistivity of antimony films. Leverton and Dekker [2] measured the electrical resistivity of thin films along with the Hall constant. Clark [3] studied the electrical conduction properties of thin films at microwave frequencies, while Coulombani *et al.* [4] studied the electrical and galvanomagnetic effects in thin films and found that when the thickness exceeded 90 nm, the properties were thickness independent. Bonfiglioli and Malvano [5] carried out field-effect studies on antimony films. The internal stress and the electrical resistivity were simultaneously measured on films during and after evaporation by Horikoshi and Tamura [6]. Chassaing [7] studied the changes in the resistance of thin films in vacuum immediately after formation. Harris and Corrigan [8] made detailed studies on the electrical conduction and Seebeck effect of thin films grown over glass and Al_2O_3 substrates at elevated temperatures and annealed. Hauser [9, 10] obtained amorphous films by deposition at low temperature and studied the conduction mechanisms in these films. Maki [11] studied the amorphous to crystalline transition in thin films by electrical conduction studies, and electrical and galvanomagnetic properties of films prepared at different substrate temperatures were reported by Barua and Barua [12]. Pal and Sen [13] analysed the size effect of the electrical conductivity on the basis of the Lucas Model [14]. Paprocki *et al.* [15] studied the galvanomagnetic properties of films, while Deschacht *et al.* [16] studied the effect of the size of crystallites on the electrical conductivity of polycrystalline films both theoretically and experimentally. Pariset [17] studied the thickness dependence of electrical conductivity of films prepared in ultra-high vacuum, in the temperature range 20 to 500 K.

Thermoelectric effects, just as electrical conduction, have been studied, to a lesser extent, to understand the transport mechanism in antimony. Harris and Corrigan [8] were the first to measure the Seebeck coefficient of antimony films at room temperature. Koike *et al.* [18] found that the Seebeck coefficient was dependent on thickness up to 500 nm. Paprocki *et al.* [15] measured the Seebeck coefficient of thin films in the temperature range 77 to 400 K and analysed their results on the basis of the theory derived by Mikolajczak *et al.* [19] taking into account the grain boundary scattering. Barua and Barua [20] studied the effect of substrate

0022–2461/89 $03.00 + .12

temperature on the Seebeck coefficient of antimony films using Mayer's [21] theory. Boyer *et al.* [22] studied the effect of grain-boundary scattering on the Seebeck coefficient of antimony films for a given thickness.

It is seen from the above that though there has been a fair amount of research, particularly on the electrical conduction in thin antimony films, there has been no work to date analysing the data on both thermoelectric power and electrical conductivity of antimony thin films taken simultaneously, except for that of Harris and Corrigan [8]. Further, the theories used to analyse the data have been older, and lacking in the incorporation of the microstructure of the films. In the present study, both the thermoelectric power data and electrical conductivity data have been analysed and the newer, effective mean free path theory developed by Tellier *et al.* [23], Tellier [24] and Pichard *et al.* [25] has been applied.

2. Experimental details

Thin films of antimony for thermoelectric power and electrical conductivity measurements were simultaneously prepared using suitable masks by vacuum deposition of bulk antimony of 99.999% purity from a molybdenum boat on to freshly cleaned glass plates held at room temperature. The source to substrate distance was about 25 cm. The glass plates were cleaned with freshly prepared warm chromic acid, Teepol detergent solution, distilled water and isopropyl alcohol in that order and then mounted inside the vacuum deposition unit for thin film preparation. The vacuum during deposition was 2×10^{-5} torr. Films of a given thickness were prepared in a single evaporation. In each deposition, a given quantity of the bulk material was taken and it was completely evaporated at a fast rate.

The film thicknesses were measured to an accuracy of ± 2 nm using a "Seavom" quartz crystal monitor. The lateral dimensions of the films were 0.5 cm $\times$ 6.5 cm for thermoelectric power measurements and 1.0 cm $\times$ 3.0 cm for electrical conductivity measurements.

After vacuum deposition, the films were annealed at 500 K for 1 h and cooled. Then the vacuum was broken and the specimens were mounted in the thermoelectric power measurement apparatus and the electrical conductivity apparatus individually, and put back into the vacuum chamber, the latter being evacuated to a pressure of 2×10^{-5} torr before making either of the measurements.

The films were annealed (at 500 K) before taking measurements as it was found from a previous study [26] that the as-grown antimony thin films have many defects (point defect clusters) as have films of most other materials [26–37], and hence show high resistivity. Upon heating (or annealing at a given temperature), some or most of the defects are annealed out (depending upon the maximum temperature of heating) so that the resistivity of the film decreases, the amount of resistivity decrease depending on the number of defects annealed out. Harris and Corrigan [8] have also found that upon heating antimony films at about 500 K, the resistivity of the films decreases by a large amount. The temperature (500 K) and the duration of heating were chosen so that almost all the point defects and clusters were removed and there was no further change in resistance because of the defect removal. Heating at a temperature above 500 K only resulted in partial evaporation of the film and consequent increase in resistance.

The integral method was employed to measure the thermal e.m.f. as a function of temperature difference. One end of the film was clamped to a massive copper heat sink and the other end could be heated with a mini heater. When the cold end was essentially at room temperature, the other end was heated to different temperatures and the thermal e.m.f. developed between the ends of the film was measured with respect to copper at different temperatures for every 2 K variation. The Seebeck coefficient, the derivative of the developed thermal e.m.f. with respect to temperature, was calculated from the above data. Both the temperature and the thermal e.m.f. measurements were made using potentiometers and sensitive null detectors (10^{-9} A/div). The thermal e.m.f. was measured to an accuracy of 1 μV.

The electrical resistance of the films was found using a Wheatstone's network. The resistance was noted as function of temperature in the range 300 to 470 K for every 2 K variation. The resistance was recorded to an accuracy of 1 Ω.

X-ray diffractograms of the films were taken. It was found that antimony films had a high degree of preferred orientation with the basal plane (in hcp lattice) parallel to the film plane as evinced by the strong (0 0 3), (0 0 6) and (0 0 9) reflections. A typical X-ray diffractogram is shown in Fig. 1.

3. Results

3.1. Thermoelectric power

Fig. 2 shows the variation of thermal e.m.f. as a function of the temperature difference for antimony films of different thicknesses with respect to copper. The developed e.m.f. is negative. Its magnitude increases monotonically with increasing temperature difference. Because the developed e.m.f. is negative, the Seebeck coefficient is positive and is determined from the data of thermal e.m.f as a function of temperature difference, by least squares error analysis using spline functions which are essentially local.

The variation of the Seebeck coefficient as a function of temperature is plotted in Fig. 3. The Seebeck coefficient is positive, temperature dependent and increases with increasing temperature. It also shows thickness dependence. It increases nonlinearly with increasing thickness. To analyse its thickness dependence, the Seebeck coefficient at 300 K was plotted as a function of inverse thickness as shown in Fig. 4. It is seen that it is inversely proportional to thickness. The best straight line, fitted by least squares error analysis, is also drawn. Fig. 4 also shows the plots of the Seebeck coefficient against the reciprocal of thickness at 350 and 400 K.

3.2. Electrical resistivity

The electrical resistivity of annealed antimony films of

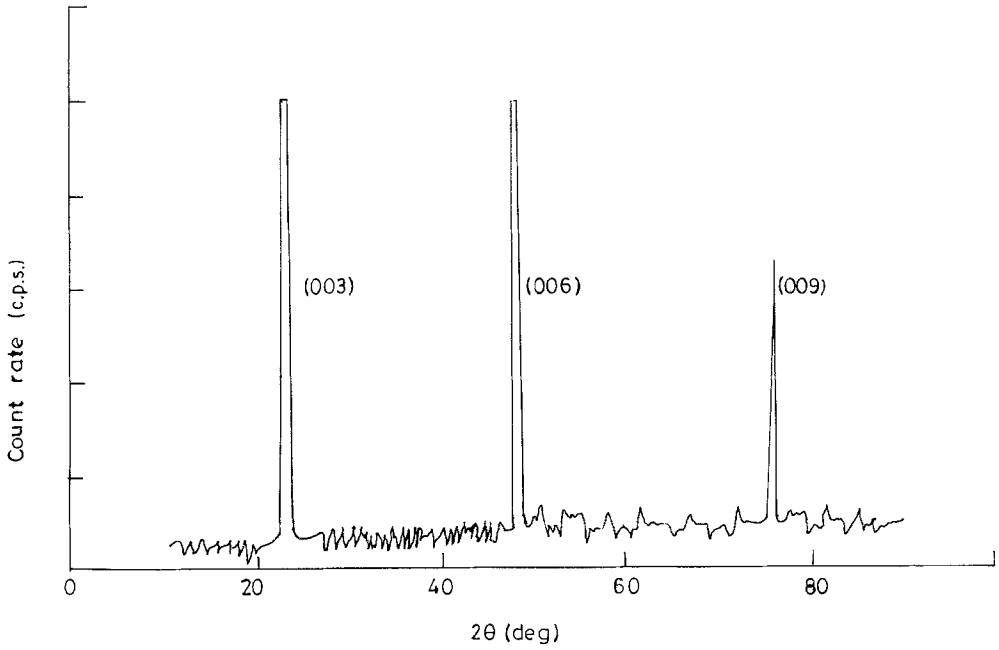

Figure 1 A typical X-ray diffractogram of antimony thin film.

different thicknesses has been measured as a function of temperature in the range 300 to 470 K. The electrical resistivity of films of different thicknesses is plotted in Fig. 5 as a function of temperature. Films show metallic behaviour. The resistivity increases with temperature, showing positive temperature coefficient of resistivity. Fig. 6 shows the thickness dependence of resistivity at 300 K: the resistivity shows a linear dependence on the reciprocal of thickness. The best fit is obtained by least squares error analysis and is shown by the straight line. Fig. 6 also shows the variation of resistivity as a function of the reciprocal of thickness at 350 and 400 K.

4. Discussion

When the properties of antimony in the thin film state are studied, in addition to the usual bulk parameters, various other new parameters (the thin film deposition parameters) should also be taken into account. It is known [38, 39] that the deposition parameters influence the structure, microstructure and defect structure of thin films and, as a consequence, the thin film properties are also influenced by the deposition parameters. Thus, research workers working on thin films of the same material often obtain different results because the deposition parameters employed by them are invariably different.

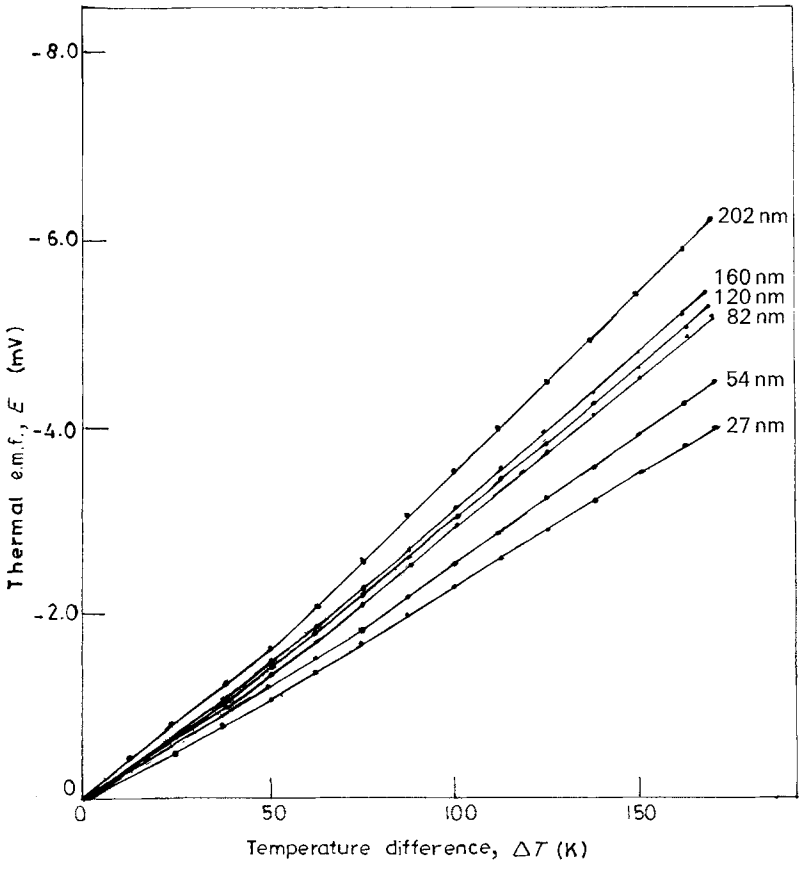

Figure 2 The variation of thermal e.m.f. as a function of temperature difference for films of different thicknesses.

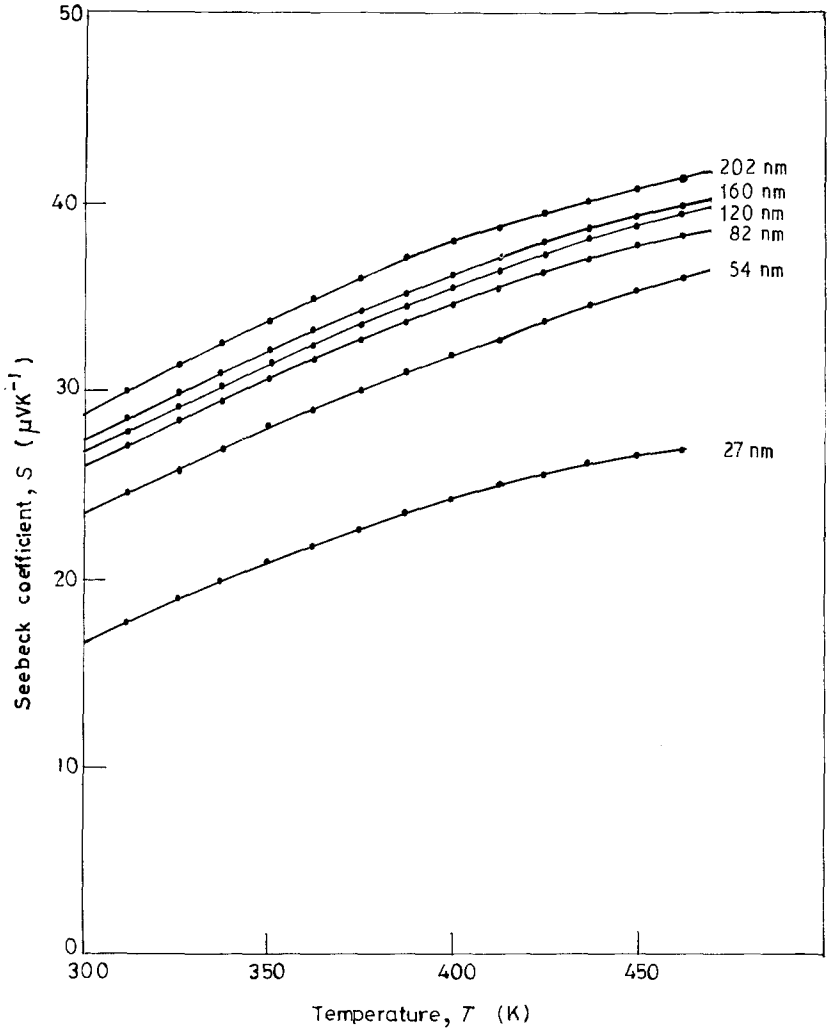

Figure 3 The variation of Seebeck coefficient as a function of temperature for films of different thicknesses.

Thin antimony films show preferred orientation whether the substrates on which they are deposited are polycrystalline or amorphous. Electron microscopic studies made by Harris and Corrigan [8] showed that the crystallites of films formed at about 400 K and annealed at about 540 K, were predominantly oriented with the trigonal axes of most of the crystallites normal to the film plane, consistent with the observations also made by Majejiko *et al.* [15].

4.1. Thermoelectric power studies

It is seen from Fig. 3 that the Seebeck coefficient of films is temperature and thickness dependent, and increases with increasing temperature and increasing thickness. The former is as expected, because the free electron theory predicts linear temperature dependence of the Seebeck coefficient for degenerate carriers. Saunders *et al.* [40, 41] found that the Seebeck coefficient of antimony increased slowly and, beyond 500 K, the Seebeck coefficient decreased. In thin films, as the mean free path of carriers is comparable to its thickness, surface scattering is another mechanism in addition to the other types of scattering. This surface scattering causes the thickness dependence of the kinetic coefficients in the thin film state. Mayer [21] was the first to show analytically that the Seebeck coefficient of thin films is thickness dependent. Normally thin films are polycrystalline. So, the grain-boundary scattering is appreciable in thin films. But in Mayer's theory this is not taken into account.

Pichard *et al.* [25] have recently developed the "effective mean free path model" using the Mayadas–Shatzkes theory [42]. In this model, grain-boundary scattering is taken into account by considering the bulk as polycrystalline, having the same grain structure as that of the films. The analytical expression in this model indicates that the Seebeck coefficient is a linear function of the reciprocal of thickness. The equation is in the free electron (spherical energy surface) approximation [43], i.e.

$$V = \left(\frac{\mathrm{d} \ln A}{\mathrm{d} \ln E}\right) E - E_F = 1$$

$$S_f = S_g\left[1 - \tfrac{3}{8}(1 - p)\frac{l_g}{t}\left(\frac{U_g}{1 + U_g}\right)\right]$$

where S_g is the Seebeck coefficient of the infinite thick film i.e. the bulk, with the grain structure of the films, l_g is the mean free path of the carriers in an infinite thick film and, $U_g = (\delta \ln l_g/\delta \ln E)_{E = E_F}$ determines the energy dependence of the mean free path of carriers in the infinite thick film. p is the specularity parameter and gives the fraction of carriers incident on surfaces that is specularly scattered by them. Generally, this is taken as zero when no knowledge about it is available from independent studies. This is because, when it is zero, the maximum effect of surface scattering, and hence the size effect, is taken into account. In the present studies also, p is taken to be equal to zero so that all the carriers are assumed to be

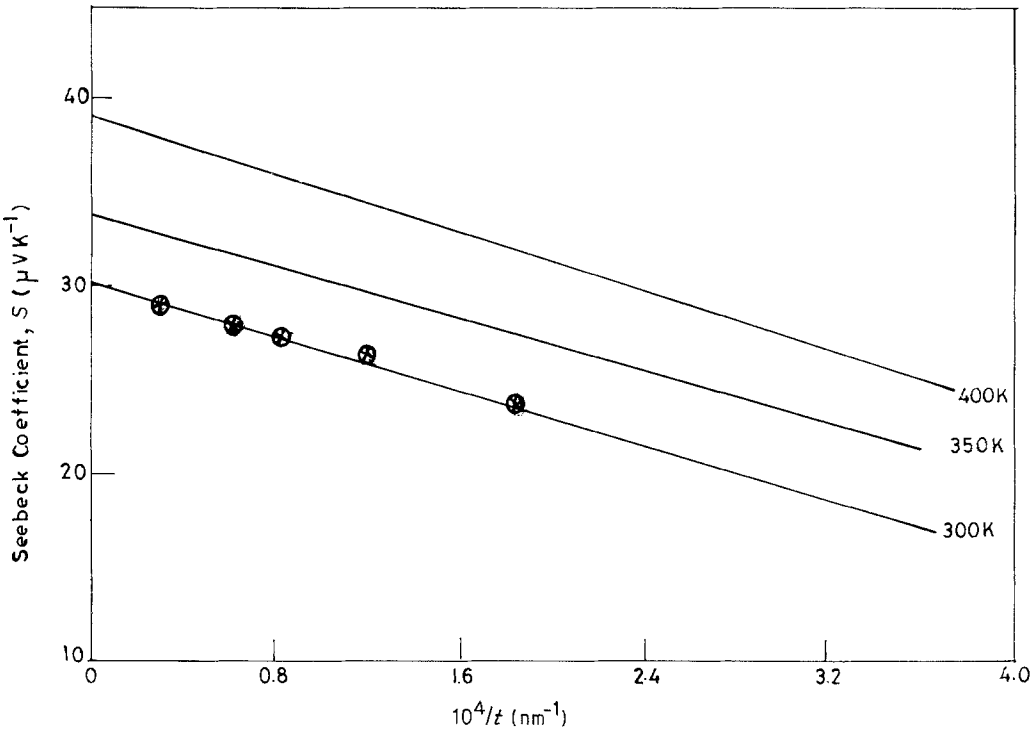

Figure 4 The thickness dependence of Seebeck coefficient at different temperatures (300, 350 and 400 K): (——) fitted lines, (x) experimental points at 300 K.

diffusely scattered from the surfaces. Harris and Corrigan [8] found from the size-effect analysis of their data using the Fuchs–Sondheimer [44] theory that the best fit was obtained for the resistivity dependence on thickness when p was adjusted to zero. Thus, our assumption of complete diffuse surface scattering is reasonable and justified. If the Seebeck coefficient of films is plotted against the reciprocal of thickness, the plot will be a straight line, the intercept will give S_g, while from the slope either l_g or $U_g = (\delta \ln l_g/\delta \ln E)_{E=E_F}$ can be determined if the other is known.

In the present studies, the data were analysed on the basis of the above effective mean free path model. In Fig. 4 the best fit for the Seebeck coefficient as a function of the reciprocal of thickness, obtained by least squares error analysis, is shown. At different temperatures (300, 350 and 400 K), the Seebeck coefficient values of the infinitely thick film are 30, 34 and 39 $\mu V K^{-1}$, respectively. Harris and Corrigan [8] found, in the case of their antimony films, that a thick film (1500 nm) had a thermoelectric power value of 45.4 $\mu V K^{-1}$ at room temperature (300 K). When their thermoelectric power data are plotted as a function of reciprocal thickness, it is found that the infinitely thick film has the Seebeck coefficient value, 44.5 $\mu V K^{-1}$. This value is about 1.5 times that of our value at the same temperature. The higher thermoelectric power of their films can be explained as due to the substrate temperature for deposition of the films being higher (~ 400 K) and thus the post-deposition annealing temperature (~ 540 K) was also higher:

(1) a higher substrate temperature causes the film crystallites to be larger so that the mean free path in the films becomes larger. This causes an increase in the thermoelectric power;

(2) further, higher substrate temperature also causes an increase in preferred orientation (texture of the film) of the crystallites.

As mentioned earlier, antimony is anisotropic because of its rhombohedral structure. The thermoelectric power of bulk single crystals in the direction of the trigonal axis is very low (21.3 $\mu V K^{-1}$) [8] compared to that in the direction normal to it (48.0 $\mu V K^{-1}$) [8, 45]. Consequently the thermoelectric power value will also increase with increasing degee of preferred orientation in the direction normal to the trigonal axis. In addition to the lower value of the infinitely thick film's thermoelectric power, in our thin films (the intercept value), it was found that the slope of S against $1/t$ is lower than that obtained from the data of Harris and Corrigan [8] (0.375×10^3 compared to 0.86×10^3 $\mu V nm K^{-1}$). It is evident from the above expression that the slope depends on both S_g and l_g (and also the energy derivative of the latter). In our case, because of the smaller crystallites, as both S_g and l_g are smaller, the slope also has to be smaller, as observed.

4.2. Electrical resistivity studies

Although the value of the mean free path of carriers is available in the literature, the direct use of it will introduce error in calculations because, as a result of defects and small grains, the mean free path in the hypothetical bulk will be different (smaller) from that of single crystals. This error can be easily avoided by studying the thickness dependence of resistivity of similar films and determining the mean free path, l_g, of the infinitely thick film having the same microstructure as that of the films studied. For this reason, films were prepared simultaneously both for resistivity and for Seebeck coefficient measurements. The temperature and thickness dependences of the resistivity of films were also determined in addition to Seebeck coefficient studies.

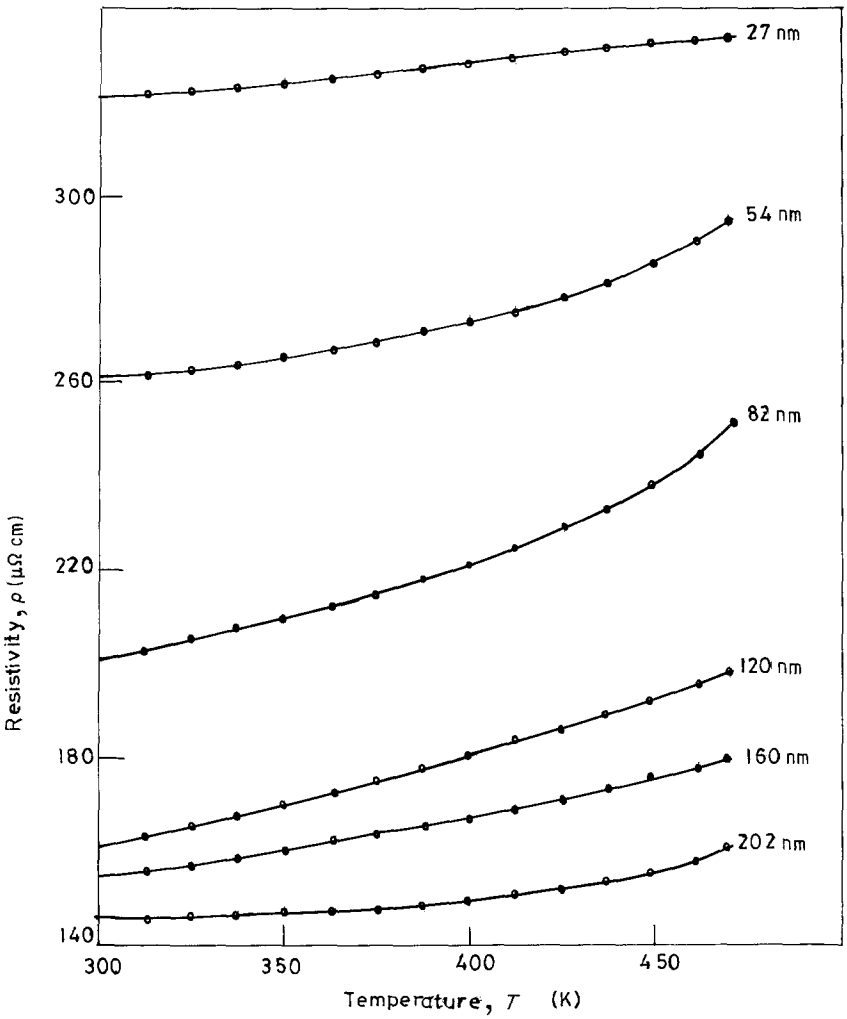

Figure 5 The variation of resistivity as a function of temperature for films of different thicknesses. (——) fitted lines, (●) experimental points at 300 K.

From Fig. 5 it is clear that all the films show metallic behaviour and the temperature coefficient of resistivity is positive. It is also evident that the resistivity is also thickness dependent. Oktu and Saunders [46] found that the resistivity of single crystals increases with increasing temperature in the range 77 to 300 K. They found that the carrier concentration remained the same but the mobility of carriers decreased with temperature. Kevitsky and Ivanov [47] measured the resistivity up to 750 K and found that it increased with temperature. Thus, the present observation of metallic behaviour of antimony thin films is in accordance with the earlier studies on bulk and single crystalline antimony.

The Fuchs-Sondheimer expression was derived [44] to analyse the thickness dependence of the resistivity taking the surface scattering into account, along with the other kinds of scattering. However, as mentioned earlier, structural studies on thin films reveal that the films are generally polycrystalline. Thus grain-boundary scattering also should be taken into account along with the surface scattering, when discussing the experimental results on film properties. The Mayadas–Shatzkes theory takes into account the grain-boundary scattering, but its expression [42] is complicated. Mola and Heras [48], Tellier *et al.* [23] and Tellier [24] attempted to simplify the analytical expressions of Mayadas–Shatzkes theory.

Tellier [24] derived a simple analytical expression for the electrical resistivity as a function of thickness by defining an effective mean free path for carriers in an infinitely thick film, a hypothetical bulk. This model is known as the effective mean path model. According to this model, the analytical expression for the film resistivity as a function of thickness is

$$\varrho_f = \varrho_g\left[1 - \frac{3}{8}\frac{(1-p)}{K_g}\right]\int_1^\infty \left(\frac{1}{x^3} - \frac{1}{x^5}\right) \times \left[\frac{1 - \exp(-x)}{1 - p\exp(-x)}\right]$$

where ϱ_g is the resistivity of the infinitely thick film, K_g is the reduced thickness (the ratio of the film thickness t, to the effective mean free path l_g).

Under asymptotic conditions, $K_g \gg 1$, the above equation of resistivity as a function of thickness becomes

$$\varrho_f = \varrho_g\left[1 + \frac{3}{8}\frac{l_g}{t}(1-p)\right]$$

It has been shown numerically that the above expression holds good down to $K_g = 0.1$, i.e. $t = 0.1\, l_g$. It is evident from the above expression that a plot of film resistivity as a function of reciprocal thickness will be linear at a given temperature.

From Fig. 6 it is clear that indeed such a plot of experimental film resistivities against reciprocal thickness is linear at 300, 350 and 400 K. We also find that the resistivity of the infinitely thick film at 300, 350 and 400 K is 125, 131 and 140 $\mu\Omega$ cm, respectively.

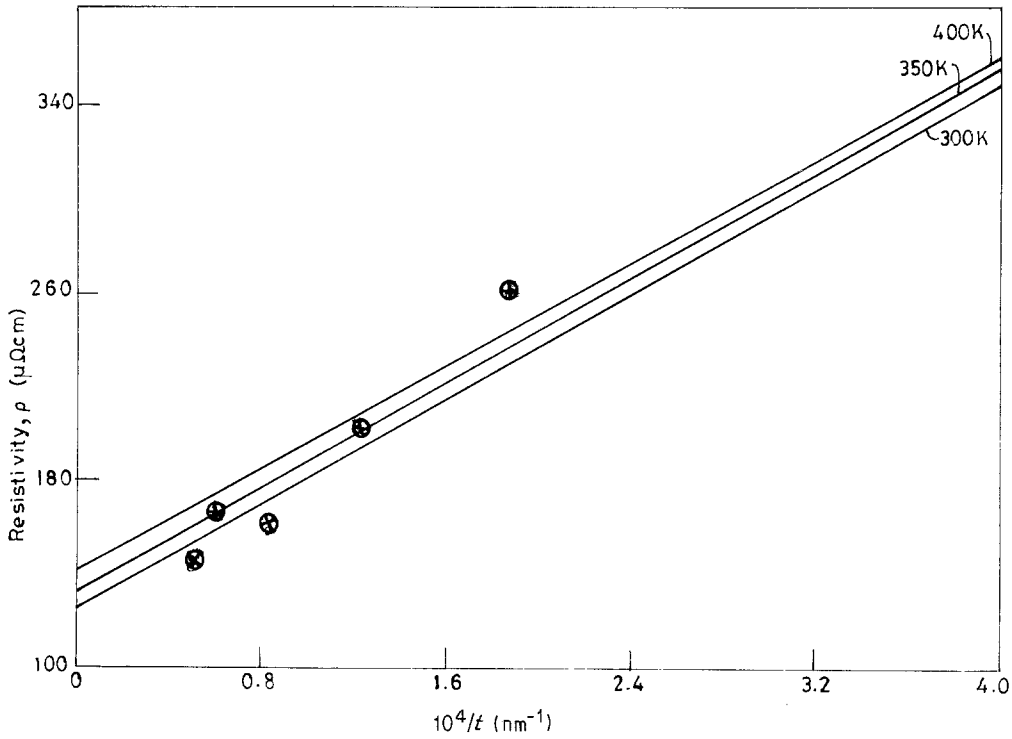

Figure 6 Plots of resistivity against the reciprocal of thickness at different temperatures (300, 350 and 400 K): (——) fitted lines, (×) experimental points at 300 K.

From the slopes of the graphs, the effective mean free path is calculated (assuming $p = 0$). The effective mean free path of carriers, l_g at 300, 350 and 400 K is 120, 114 and 105 nm, respectively. These values are to be compared with the value of the mean free path obtained by thin film resistivity size effect analysis by Paprocki *et al.* [15], namely 700 nm (at 273 K): our values are lower by a factor of about six compared to their value. The reason for this is that they have used the older Fuchs–Sondheimer [44] theory for the analysis of thickness dependence of the resistivity which does not take account of grain-boundary scattering. In fact, Paprocki *et al.* [15] have also analysed the size dependence of thermoelectric power of similar antimony films, but based on a theory (by Mikolajczak *et al.* [19]) which also takes into account the grain-boundary scattering of carriers. From this, they obtain the value 300 nm (at 273 K) which is less than half the value obtained from their resistivity data. The bulk mean path value obtained by Harris and Corrigan [8] is ony 153 nm (at 300 K) in contrast. Thus, evidently, taking into consideration grain-boundary scattering makes a very considerable difference (for the better) to the obtained mean free path value.

4.3. Combined analysis of ϱ and α data

Mayadas–Shatzkes showed that the presence of the grain-boundary scattering reduces the mean free path of carriers thereby resulting in an increase in resistivity. They showed that $\varrho_g l_g = \varrho_0 l_0$ where ϱ_g and l_g are the resistivity and the mean free path of carriers in the bulk with film microstructure, and ϱ_0 and l_0 are the resistivity and the mean free path of carriers in a single crystal. Thus, according to the free electron theory

$$\frac{1}{\varrho_0 l_0} = \left(\frac{1}{3\pi^2}\right)^{1/3} \frac{e^2 n^{2/3}}{\hbar} = \frac{1}{\varrho_g l_g}$$

where $\hbar = h/2\pi$ and h is Planck's constant, and e is the electronic charge. ϱ_g and l_g can be estimated from the resistivity data analysis, and the carrier concentration, n, calculated at different temperatures. At 300, 350 and 400 K the calculated values of the carrier concentration are 2.4×10^{19}, 2.4×10^{19} and 2.5×10^{19} carriers/cm^3. Thus, the carrier concentration is independent of temperature, and degenerate. This observation agrees with the earlier observation of Oktu and Saunders [46] that the carrier concentration of antimony is constant and the resistivity change with temperature is due to change in mobility. The carrier concentration estimated by others, below 300 K, varies from 3.9 to 5.5×10^{19} carriers/cm^3. Using the value of the "grain boundary" mean free path, l_g, obtained at different temperatures from the ϱ_f against $1/t$ plots in the expression for the slopes of the S_f against $1/t$ plots at different temperatures, the parameter $U_g = (\mathrm{d} \ln l_g/\mathrm{d} \ln E)_{E = E_F}$ was calculated at temperatures 300, 350 and 400 K. The values are 0.36, 0.32 and 0.33, respectively.

It may be pointed out here that using the values of U_g above, it is possible to evaluate the values of $U = (\mathrm{d} \ln l_0/\mathrm{d} \ln E)_{E = E_F}$ using the simple relation $U_g = U\sigma_g/\sigma_0 = U\varrho_0/\varrho_g$ where ϱ_g is the grain-boundary resistivity and ϱ_0 the bulk single crystalline resistivity at the desired temperature. Also the values of the parameter V (which has been assumed to be 1 in the present study, according to spherical Fermi surface approximation) can be calculated from the intercepts of the S_f against $1/t$ plots using the relation

$$\text{intercept} = S_g = \frac{-\pi^2 k^2 T}{3eE_F}(V/U_g)$$

at different temperatures, if the value of E_f is known.

However, the values of σ_0 and E_F available in the literature vary by large amounts (perhaps because of

TABLE I Values of thermoelectric power, S_g, resistivity, ϱ_g, mean free path, l_g, of the infinitely thick film, U_g and, carrier concentration, n, Fermi energy, E_F and effective mass, m^*, in antimony determined at different temperatures, compared with earlier values

Temperature (K)	S_g or S_0 ($\mu V K^{-1}$)	ϱ_g or ϱ_0 ($\mu\Omega$ cm)	l_g (nm)	Carrier concentration (cm^{-3})	U_g = (d ln l_g/d ln $E)_{E=E_F}$	Fermi energy (eV)	Effective mass (m_0)
				(a) Present study values			
300	30	125	120	2.37×10^{19}	0.36	0.33	0.09
350	34	131	114	2.40×10^{19}	0.32	0.28	0.11
400	39	140	105	2.45×10^{19}	0.33	0.25	0.12
				(b) Data from earlier studies			
300	44.5 [8]	56.5 [8]	153 [8]	3.9 to 5.5×10^{19}		0.14 [26] 0.18 [15] 0.080 [51]	0.084 [49, 50] (electron) 0.124 (holes)
273			700 [15] 300				

anisotropy). Also, no information is available about the value of σ_0 at different temperatures. Hence, it was decided not to use any values from the literature and make the calculations in the present study, self-contained, but assuming $V = 1$, i.e. spherical Fermi surface approximation (free electron approximation).

The Seebeck coefficient of an infinitely thick film is given by

$$S_g = \frac{-\pi^2 k^2 T}{3eE_F}(1 + U_g)$$

using $V = 1$ in the free electron approximation. Using this expression, the Fermi energy values of holes have been determined as 0.33, 0.28 and 0.25 eV at 300, 350 and 400 K.

As the Fermi energy and the carrier concentration are calculated from the analysis of results, these values can be used to determine the effective mass of carriers in the expression

$$E_F = \frac{\hbar^2}{2m^*}(3\pi^2 n)^{2/3}$$

The effective mass (m^*) calculated is 0.09, 0.11 and 0.12 times the rest electron mass, at temperatures 300, 350 and 400 K, respectively. Thus, the effective mass of the carriers is temperature dependent. All the calculated parameters are given in Table I with earlier data for comparison.

5. Conclusions

Thin antimony films of different thicknesses ranging from 30 to 200 nm were prepared. The Seebeck coefficient and the electrical resistivity of these specimens were found in the temperature range from 300 to 470 K, after annealing the films at 500 K for about an hour. The X-ray studies revealed that the films were preferentially oriented with the trigonal axes of the grains normal to the film plane. The Seebeck coefficient and the resistivity of films increased with increasing temperature, confirming that the carriers are degenerate. The experimental results were analysed on the basis of the effective mean free path model developed by Tellier and Pichard *et al.* It is seen that the analysis of the Seebeck coefficient and resistivity data not only explains the thickness dependence of the Seebeck coefficient and the electrical resistivity of thin films, but also leads to the estimation of parameters such as the Fermi energy, the carrier concentration, the effective mass of the carriers and the parameter, U_g.

References

1. LOUIS HARRIS and L. H. SHAFFER, *Phys. Rev.* **76** (1949) 943.
2. W. F. LEVERTON and A. J. DEKKER, *Phys. Rev.* **80** (1950) 732.
3. D. N. CLARK, *Brit. J. Appl. Phys.* **6** (1955) 158.
4. A. COULOMBANI, C. VANTIER and P. HUET, *C. R. Acad. Sci.* **247** (1958) 1838.
5. G. BONFIGLIOLI and R. MALVANO, *Phys. Rev.* **115** (1959) 330.
6. H. HORIKOSHI and N. TAMURA, *Jpn J. Appl. Phys.* **2** (1963) 328.
7. G. CHASSAING, *C. R. Acad. Sci.* **258** (1964) 4009.
8. L. HARRIS and F. R. CORRIGAN, *J. Phys. Chem. Solids* **26** (1965) 307.
9. J. J. HAUSER, *Phys. Rev. B* **9** (1974) 2623.
10. *Idem, ibid.* **11** (1975) 738.
11. K. MAKI, *Jpn. J. Appl. Phys. Suppl.* **2** (1974) 649.
12. D. C. BARUA and K. BARUA, *Ind. J. Phys.* **49** (1975) 603.
13. A. K. PAL and P. SEN, *J. Mater. Sci.* **10** (1975) 1879.
14. M. S. P. LUCAS, *J. Appl. Phys.* **36** (1965) 1632.
15. K. POPROCKI, K. MAJEJKO, M. SUBOTOWICZ and M. JALACHOWSKI, *Thin Solid Films* **36** (1976) 93.
16. D. DESCHACT, A. BOYER and E. GROUBERT, *ibid.* **70** (1980) 311.
17. C. PARISET, *ibid.* **91** (1982) 301.
18. R. KOIKE, H. KUROKAWA and Y. IIJIMA, *Jpn J. Appl. Phys.* **7** (1968) 293.
19. P. MIKOLAJCZAK, W. PIASEK and M. SUBOTOWICZ, *Phys. Status Solidi (a)* **25** (1974) 619.
20. K. BARUA and D. C. BARUA, *Ind. J. Pure Appl. Phys.* **14** (1976) 496.
21. H. MAYER, "Structure and Properties of thin films", edited by C. A. Neugebauer, J. B. Newkirk and D. A. Vermilyea, (Wiley, New York, 1959) p. 225.
22. A. BOYER, D. DESCHACHT and E. GROUBERT, *Thin Solid Films* **76** (1981) 119.
23. C. R. TELLIER, A. J. TOSSER and C. BOUTRIT, *ibid.* **44** (1978) 201.
24. C. R. TELLIER, *ibid.* **51** (1978) 311.
25. C. R. PICHARD, C. R. TELLIER and A. J. TOSSER, *J. Phys. F. Metal Phys.* **10** (1980) 2009.
26. V. DAMODARA DAS and M. S. JAGADEESH, *Nucl. Phys. Solid State Phys. (Ind.)* **17C** (1974) 139.
27. V. DAMODARA DAS and N. JAYAPRAKASH, *Phys. Status Solidi (a)* **68** (2) (1981) K159.
28. V. DAMODARA DAS and N. JAYAPRAKASH, *J. Vac. Sci. Technol* **20** (1982) 58.
29. *Idem, J. Mater. Sci.* **17** (1982) 1369.
30. V. DAMODARA DAS and H. UDAYA KUMAR, Pro-

ceedings 7th IVC and 3rd ICSS (Vienna) Vol. 3, (1977) pp. 1675–78.
31. V. DAMODARA DAS and A. ANAND S. TALWAI, *Thin Solid Films* **81** (1981) 21.
32. V. DAMODARA DAS and M. S. JAGADEESH, *ibid.* **24** (1974) 203.
33. *Idem, J. Phys. Chem. Solids* **38** (1977) 167.
34. M. S. JAGADEESH and V. DAMODARA DAS, Proceedings 7th IVC and 3rd ICSS (Vienna) Vol. 3, (1977) pp. 1935–38.
35. V. DAMODARA DAS and M. S. JAGADEESH, *J. Mater. Sci.* **17** (1982) 671.
36. V. VAND, *Proc. Phys. Soc.* **55** (1942) 222.
37. V. DAMODARA DAS, *J. Appl. Phys.* **55** (1983) 1023.
38. L. I. MAISSEL and R. GLAG, "Handbook of Thin Film Technology" (McGraw Hill, New York, 1970).
39. K. L. CHOPRA, "Thin Film Phenomena" (McGraw Hill, New York, 1969).
40. G. A. SAUNDERS and O. OKTU, *J. Phys. Chem. Solids* **29** (1968) 327.
41. G. A. SAUNDERS, C. MIZIUMSKII, G. S. COOPER and A. W. LAWSON, *J. Phys. Chem. Solids* **26** (1965) 1299.
42. A. F. MAYADAS and M. SHATZKES, *Phys. Rev. B* **1** (1970) 1382.
43. C. R. TELLIER and A. J. TOSSER, *Thin Solid Films* **41** (1977) 161.
44. E. H. SONDHEIMER, *ibid.* **18** (1973) 137.
45. P. W. BRIDGMAN, Proc. Amer. Acad. Arts Sci. 63 (1929) 351.
46. O. OKTU and G. A. SAUNDERS, *Proc. Phys. Soc.* **91** (1967) 156.
47. YU. KEVITSKVY and T. G. AIVANOV, *Fiz. Metallov Metalloved.* **27** (1969) 598.
48. E. E. MOLA and J. M. HERAS, *Thin Solid Films* **18** (1973) 137.
49. L. R. WINDMILLER, *Phys. Rev.* **149** (1966) 472.
50. J. E. PARROT, *Proc. Phys. Soc. London* **85** (1965) 1143.
51. J. J. HAUSER and L. R. TESTARDI, *Phys. Rev. Lett.* **20** (1968) 12.

Received 26 January 1988
and accepted 11 January 1989